linearized in R,

$$O(t)=[\omega R/(\omega R+B)][e^{-(\Delta-t)}\{1-R[(1-\omega)(1+t)+2\omega e^{-(\Delta-t)}]\}+R(1-\omega)+\omega e^{-(\Delta-t)}]$$
$$+[B/(\omega R+B)]R[(1-\omega)+\omega e^{-(\Delta-t)}],\quad 0\leqslant t\leqslant\Delta;\quad O(t)=B/(\omega R+B),\quad t>\Delta. \quad \text{(AI17)}$$

We have omitted from consideration the $e\mu'\mu$ events for which μ' occurs within the dead-time of a previous analysis, since such events contribute only terms of order R^2 to the total distribution.

APPENDIX II

In applying Peierls' method for determining lifetime,[21] one needs to know the mean time $\bar{t}_n$ of events in the nth channel. Due to the finite channel width d, $\bar{t}_n \neq t_n$, the channel midpoint, but one has instead,

$$t_n-\bar{t}_n=\int_{-\infty}^{\infty} sp_n(s)ds \Big/ \int_{-\infty}^{\infty} p_n(s)ds,\quad s\equiv t-t_n, \quad \text{(AII1)}$$

where $p_n(s)$ is the relative probability for an event to occur at time t and be stored in the nth channel. $p_n(s)$ is clearly the product of $O(t)$, the output time distribution of events, and $R_n(s)$, the channel resolution. $R_n(s)$ is the probability for an interval of length t to be sorted into the nth channel. Therefore,

$$\bar{t}_n-t_n=\int_{-\infty}^{\infty} sO(s+t_n)R_n(s)ds \Big/ \int_{-\infty}^{\infty} O(s+t_n)R_n(s)ds. \quad \text{(AII2)}$$

$R_n(s)$ can be determined empirically by means of pairs of "delta" pulses of varying separation. For the digitron used here it has, both in theory and in practice, the triangular form (independent of n)

$$\begin{aligned} R(s)&=(d+s)/d^2, && -d\leqslant s\leqslant 0,\\ &=(d-s)/d^2, && 0\leqslant s\leqslant d,\\ &=0, && \text{otherwise.}\end{aligned} \quad \text{(AII3)}$$

In the absence of background, (or subtracting it before analysis), $O(t)=e^{-t}$. Using Eq. (AII2), this gives

$$\bar{t}_n-t_n=d^2/6+\text{order}(d^4). \quad \text{(AII4)}$$

Peierls assumes that $R(s)$ has the "box-like" form

$$\begin{aligned} R(s)&=1/d, && -d/2\leqslant s\leqslant d/2,\\ &=0, && \text{otherwise,}\end{aligned} \quad \text{(AII5)}$$

which gives

$$\bar{t}_n-t_n=d^2/12. \quad \text{(AII6)}$$

For most of our measurements, $d\simeq 0.1$, so that it was important to use the pertinent expression, i.e., (AII6) rather than (AII4).

PHYSICAL REVIEW VOLUME 125, NUMBER 5 MARCH 1, 1962

Measurement of Total Cross Sections of K^- Mesons in Hydrogen and Deuterium in the Momentum Region 630 to 1100 Mev/c*

O. CHAMBERLAIN, K. M. CROWE, D. KEEFE, L. T. KERTH, A. LEMONICK,† TIN MAUNG, AND T. F. ZIPF
Lawrence Radiation Laboratory, University of California, Berkeley, California

(Received October 16, 1961)

Total cross sections of K^- mesons in hydrogen and deuterium were measured over the momentum range 630 to 1100 Mev/c. The K^-—n total cross sections were obtained from deuterium and hydrogen data. A well-defined resonance appeared in the K^-—p total cross section at about 1000 Mev/c. Two high-resolution velocity-selecting Čerenkov counters were used to select K^- mesons. The momentum resolution was within 1% to 2%, and the momentum intervals chosen were very closely spaced.

I. INTRODUCTION

In a recent experiment Cook *et al.*[1] have made an extensive study of the behavior of the K^--meson cross sections on protons (σ_p) and neutrons (σ_n) in the momentum region 1 to 4 Bev/c. They have shown the existence of structure in σ_p and, in particular, evidence for variations in the behavior of the isotopic spin components $I=1$ and $I=0$. At low energies, measurements of total cross sections from emulsion and bubble chamber work[2] show that for momenta below a few

* Work done under the auspices of the U. S. Atomic Energy Commission.

† Present address: Palmer Physical Laboratory, Princeton University, Princeton, New Jersey.

[1] V. Cook, B. Cork, T. F. Hoang, D. Keefe, L. T. Kerth, W. A. Wenzel, and T. F. Zipf, Phys. Rev. **123**, 320 (1961).

[2] L. W. Alvarez, *Ninth International Conference on High-Energy Physics, Kiev, 1959* (Academy of Sciences, Moscow, 1960), Plenary Session I–V, p. 471. See also L. W. Alvarez, University of California, Lawrence Radiation Report UCRL-9354, 1960 (unpublished).

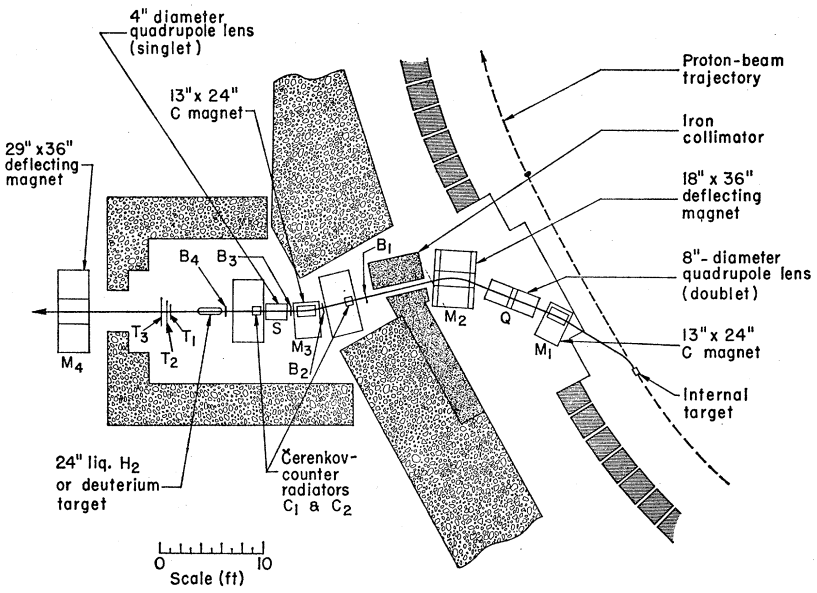

FIG. 1. Arrangement of the secondary K^- beam. M_1, M_2, and M_3 are bending magnets defining the momentum, Q is a quadrupole doublet lens, and S is a quadrupole singlet lens. The scintillation counters B_1, B_2, B_3, and B_4 define the beam and T_1, T_2, and T_3 measure the transmission of the hydrogen target.

hundred Mev/c, σ_p roughly follows a $1/v$ law. This dependence has been described elegantly and in detail by Dalitz and Tuan,[3] who assumed a dominantly S-wave interaction. Although there are some data on the absorption process of K^- mesons on neutrons, there is no information on σ_n at these low energies. The object of this experiment was to measure σ_p and σ_n near 1 Bev/c, at the lower end of the region studied by Cook *et al.*,[1] but with considerably higher momentum resolution and at more closely spaced intervals; and also to explore further the hiatus between the high-energy counter and the low-energy bubble chamber and emulsion observations. Thus, between the momenta 630 and 1100 Mev/c, σ_p was measured at nine and σ_n at five values of incident momentum. The momentum width chosen (between 1 and 2%) was about one-fifth as large as that in the experiment of Cook *et al.*,[1] and although the counting rate was correspondingly smaller, it was possible thereby to study finer details of the structure in the cross sections.

II. BEAM AND EXPERIMENTAL EQUIPMENT

A. The K^- Beam

Figure 1 shows the arrangement of counters and magnets used to obtain a variable-energy K^--meson beam of narrow momentum width. The primary target was of stainless steel, $6\times\frac{1}{2}\times\frac{1}{4}$ in. located in the magnet gap of the Bevatron. Negative particles, produced within a few degrees of the direction of the circulating proton beam, entered the channel after passing through a 0.020-in. aluminum window in the vacuum tank at the beginning of the west straight section. The first bending magnet M_1 was used to correct for variation in the apparent target position with selected momentum. For particles at the center of the momentum interval accepted, a horizontal image of the Bevatron target was formed by the quadrupole doublet Q at the center of the quadrupole-singlet field lens S. A vertical image of the target was formed at the counters T_1, T_2, and T_3 by the combination of Q and S. The operating momentum of the system was defined primarily by M_2. The main function of M_3 was to remove degraded particles from the beam. A calibration of the operating momentum was obtained by use of the floating-wire technique with all three bending magnets in their final locations. A more precise value of the momentum—and in addition, the momentum spread—was obtained by using a 29×36-in. deflecting magnet downstream of the apparatus [see Sec. II(C)]. The measured momentum spread was between 1 and 2% for all momenta.

Two velocity-selecting coincidence-anticoincidence Čerenkov counters with the two scintillation-counter pairs B_1–B_3 and B_2–B_4 were used to select the K^- mesons in the beam and to reject π^- mesons, μ^- mesons, electrons, and antiprotons. The time delays between B_1 and B_3 and between B_2 and B_4 were adjusted so that some velocity discrimination between K^- mesons and π^- mesons was possible. This was more effective at the lower momenta than at the higher. At all momenta antiprotons were rejected by this means.

The target flask, made from 0.010-in. Mylar, was 24 in. long and 6 in. in diameter. It was of the standard vacuum-insulated type with a 0.002-in. aluminized-Mylar heat shield. The vacuum jacket was made of aluminum with a 0.035-in. Mylar entrance window and a 0.032-in. aluminum exit dome. The flask could be filled with either deuterium or hydrogen.

[3] R. H. Dalitz and S. F. Tuan, Ann. Phys. 8, 100 (1959).

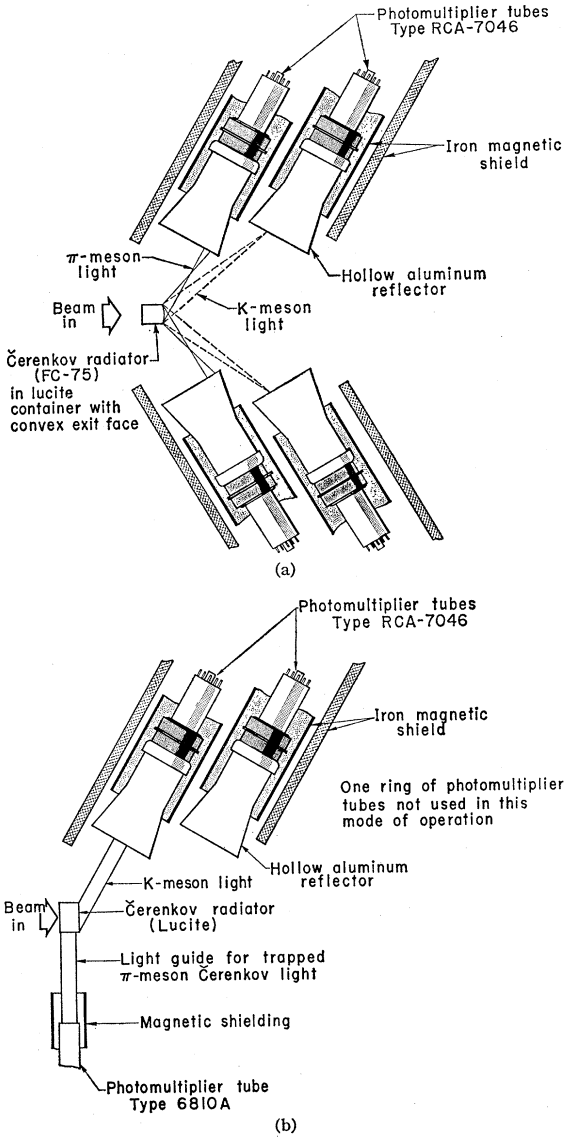

FIG. 2. Operation of the velocity-selecting Čerenkov counters. Figure 2(a) shows the mode of operation in which both the K light and π light leave the exit face of the radiator and are collected by identical photomultiplier rings, each composed of six RCA 7046 tubes. Figure 2(b) shows the mode in which the K light leaves the exit face and the trapped π light is collected through a Lucite light pipe in optical contact with the circular edge of the radiator.

B. Čerenkov Counters for Selecting K^- Mesons

The Čerenkov counters are similar to the narrow-band velocity-selecting type described by Wiegand[4] (see Fig. 2). Note that these counters not only provide a "yes" signal when a K meson passes through, but also provide a "no" signal when a lighter particle traverses the radiator. Counter C_1 is located after the primary momentum-selecting magnet M_2, whereas C_2 is placed after M_3. The radiators are right-circular cylinders with axes parallel to the beam direction. For momenta from 600 to 800 Mev/c, a Lucite radiator was employed; at higher momenta the radiator was liquid Fluorochemical (FC 75). A particle of velocity β traveling parallel to the axis produces a cone of Čerenkov light of half angle θ_c, given by $\cos\theta_c=1/n\beta$, where n is the refractive index of the radiator. The light produced by the K mesons of the correct momentum leaves the downstream end of the radiator and is refracted at this surface to a wider angle θ_r. This light is then transmitted by specular reflection down an aluminum light pipe to the photocathode of an RCA 7046 photomultiplier tube. Light leaving the radiator at angles greater than θ_r is prevented from entering this light pipe by a circular baffle. There are, at this angle, six such light pipes and photomultipliers placed in a ring about the beam axis. These six channels are divided into two groups of three each. A coincidence between the signals from the two groups must be formed in order that a K meson be counted. Lighter particles produce Čerenkov light at a larger angle than does a K meson of the same momentum. For momenta above 800 Mev/c this light leaves the end window of the radiator at an angle greater than that for the K light, and is collected by light pipes similar to those used to collect the K light. Again there are six light pipes and photomultipliers placed in a ring about the beam axis. The entrance apertures of these light pipes are positioned in such a way that they intercept light leaving the radiator at angles larger than those corresponding to the K light. For the anticoincidence signal, the pulses from the photomultipliers are added together. In this way a signal from any one of the six photomultipliers in a single counter unit can give an anticoincidence pulse that will reject the unwanted light particles [see Fig. 2(a)]. For the momentum range from 600 to 800 Mev/c, the angle of the Čerenkov light from the light particles is such that it always strikes the end face of the Lucite radiator at an angle greater than the critical angle, and hence is trapped in the radiator. This light is collected by a single light pipe in optical contact with one of the side walls of the radiator, and is transported to the photocathode of an RCA 6810-A photomultiplier. The signal from this tube then provides the anticoincidence signal [see Fig. 2(b)].

Figure 3 shows a delay curve obtained when the delays of scintillators B_3 and B_4 were varied with respect to all other counters in the system. The K mesons are counted with a time-resolution curve, indicated by the central peak. This rate corresponds to about 2×10^{-3} of the π-meson rate, and the full width at half maximum of the timing curve is 10 mμsec. If the timing is off by a large amount, say 50 mμsec, then the K mesons selected by the Čerenkov counters are never counted by the scintillators. However, there is a steady background, at about 1% of the

[4] C. Wiegand, I.R.E. Trans. on Nuclear Sci. **NS-5**, 77 (1958).

K rate, that is due to accidental coincidences of light mesons in the beam. When the delay is only about ± 10 to ± 20 mμsec, the anticoincidence pulse produced by the off-time particle in the Čerenkov counters results in a reduction of the accidental rate by more than an order of magnitude. Thus, very fast time resolution is not required for the transmission-counter coincidence circuit, because the background accidental rate is less by roughly three orders of magnitude than the K rate for delay times of ± 20 mμsec about the arrival time of the K meson.

C. Beam Purity and Momentum Measurements

To confirm the method of identification described previously, the time of flight of those particles identified as K mesons was compared with the π-meson time of flight. This was done by displaying on a recording oscilloscope the pulse from the first counter in the beam B_1 and the pulse from a counter T_F placed a known distance downstream. The oscilloscope was triggered during one series of runs by the "K" signal obtained by using the Čerenkov counters and then, during another series, by a π signal generated by B_1, B_2, B_3, and B_4 with the Čerenkov counters turned off. Thus the difference in time of flight between π^- mesons and the presumed K^- mesons was determined at several representative momenta. The results not only indicated that the K mesons were being correctly identified but also that the π contamination in the K signal to the transmission-counter coincidence circuit was less than 0.5%.

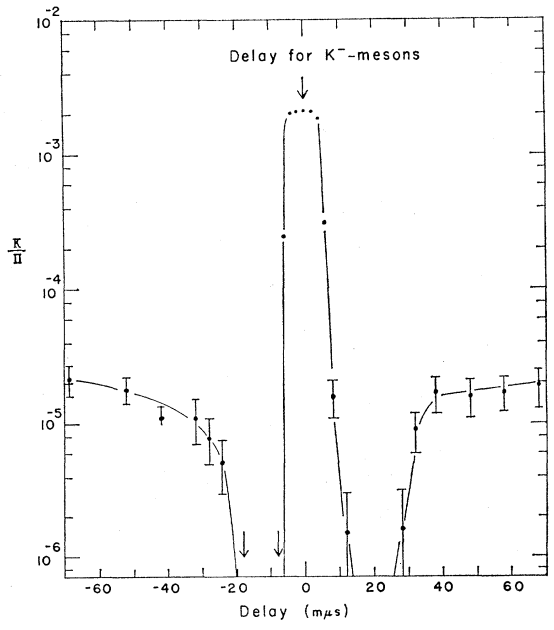

FIG. 3. Delay curve obtained by delaying B_3 and B_4 in the main K-selecting coincidence circuits. This illustrates the effectiveness of the anticoincidence signals from the Čerenkov counters in suppressing accidental coincidences that occur within about ± 20 mμsec of the passage of a K meson.

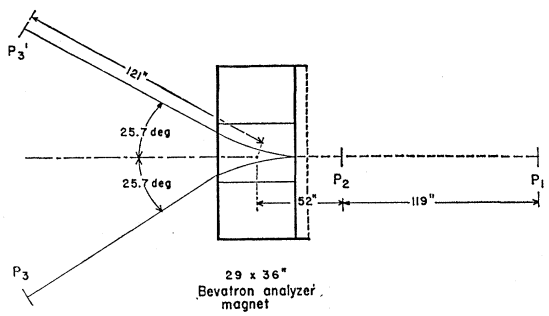

FIG. 4. Arrangement of bending magnet and counters placed downstream from the experiment to measure the beam momentum. P_1, P_2, P_3, and P_3' are vertical strip scintillation counters each $6\times\frac{1}{2}\times\frac{1}{8}$ in. Coincidences P_1, P_2, and P_3 are measured for one sign of the field in the magnet and coincidences P_1, P_2, and P_3' for the reversed field.

A precise and independent measurement of the beam momentum at the location of the hydrogen target was made (see Fig. 4) by using a telescope of two vertical strip scintillation counters P_1 and P_2 to define the direction of entrance into the 29×36-in. bending magnet, and a similar counter P_3 behind the magnet to determine the angle of deflection. These three defining counters were each $6\times\frac{1}{2}\times\frac{1}{8}$ in.; P_1 was placed upstream of the hydrogen target, P_2 close to the magnet, and P_3 about 10 ft behind the bending point. The central momentum and the spread in momentum were determined by studying the threefold coincidence rate as a function of the magnet current. The magnet was calibrated *in situ* by using the floating-wire method. Possible systematic asymmetries due, for example, to the Bevatron stray field or to hysteresis effects were eliminated by reversed-field measurements by using P_3', the image counter of P_3 in the beam line. In all cases the central momentum was determined to within 1%.

III. RESULTS

The total cross sections in hydrogen and deuterium were measured by making transmission measurements on the full and empty target. At each momentum several runs were made with the target alternately full and empty; a total of about 10^5 incident K^- mesons was recorded. To measure the transmission, three scintillation counters of different sizes were placed about 40 in. behind the target and coaxial with it. The two smaller circular transmission counters were 7 and 9 in. in diameter, respectively; the third was a square 13×13-in. counter. Thus each counter subtended different solid angles at the target.

If t_F and t_E are the transmission factors for the full and empty target, respectively, then the cross section is given by $\sigma=(1/nL)\ln(t_E/t_F)$, where L is the length of the target, and n is the difference between the atomic concentrations of the liquid in the full target and the gas in the empty target. The value of t_E was

TABLE I. Total cross sections σ_p and σ_d. The σ_n given below are obtained from hydrogen-deuterium subtraction by applying Glauber's correction. (The values are plotted in Fig. 5.)

K^--p total cross sections									
p (Mev/c)	630	752	840	894	931	987	1030	1067	1101
σ_p (mb)	35.4±3.0	36.4±2.5	36.1±1.7	42.7±2.2	44.1±1.8	45.3±2.1	48.4±1.8	49.4±2.0	44.5±1.5
K^--d and K^--n total cross sections									
p (Mev/c)	627	750	808	984	1067				
σ_d (mb)	59.1±3.4	64.5±2.5	63.1±2.3	80.9±2.1	81.0±1.3				
σ_n (mb)	26.2±4.9	31.2±4.0	30.0±3.2	40.7±3.2	36.6±2.6				

about 0.70 at the lowest momentum and 0.85 at the highest, whereas the ratio t_E/t_F was typically about 1.15 for hydrogen and 1.19 for deuterium.

The subtraction of full and empty target data does not exactly cancel all background effects, therefore the corrections listed below were applied to the measured numbers before the final results listed in Table I were obtained.

(a) *Forward scattering.* In the absence of any data on the real part of the forward scattering amplitude the differential-scattering cross section per unit solid angle in the forward direction was assumed to be equal to the lower limit $(k\sigma/4\pi)^2$ given by the optical theorem, where k is the wave number corresponding to the momentum considered. In the worst case the correction for hydrogen was less than 1 mb for the smallest counter and less than 4 mb for the largest. This correction would have to be revised if the real part of the forward scattering amplitude were found to be comparable with the imaginary part in this energy region. This correction was multiplied by a factor of approximately 1.1 to take account of double scattering in the hydrogen and in the aluminum jacket of the target.

(b) *Decays in flight.* At the momenta studied, a considerable fraction of the K^- mesons undergo decay in flight between the last Čerenkov counter and the transmission counters. In the lowest order the effect is removed by taking the target-full and target-empty difference, but three higher-order corrections need to be applied. The largest of these arises from the energy degradation in the full target, which enhances slightly the rate of decay between the target and transmission counters. The other two corrections involve the small fraction of decay products that strike the counters and simulate a K^--meson count; those occurring ahead of or within the target suffer some attenuation in the full target, whereas those occurring later have a slightly increased chance of counting because the K-meson has been slowed down in the liquid hydrogen. Since all the pertinent parameters are well known, this correction can be calculated exactly; it varies from about 3.5 mb for the lowest momentum to about 0.3 mb at the highest momentum.

(c) *Accidental counts and rate sensitivity.* The delay curve shown in Fig. 3 illustrates the effect of the Čerenkov-counter anticoincidence counting in suppressing off-time accidental counts that could arrive within the resolution time of the transmission counters. Another source of accidental background arose from particles that passed outside the Čerenkov counters, and so did not have this protection. The origin and rates of accidental counts were fully studied by using various counter combinations and different beam levels; this accidental rate was monitored continuously. The average correction was 2 mb for the largest counter and 1 mb for the smaller counters.

(d) *Beam divergence.* Beam-profile measurements were made at each momentum setting. When the target is full, Coulomb scattering in the hydrogen or deuterium increases the size of the focal spot; at the lowest momentum for the smallest counter this results in a correction of about 1 mb. For the larger counters and higher momenta the correction is negligible. The above corrections were applied for both the hydrogen and deuterium data.

In arriving at the cross section appropriate to free neutrons the following correction was applied.

(e) *Screening effect in the deuteron.* Glauber[5] has shown that the cross section on the neutron, σ_n, may be obtained from the cross sections σ_d and σ_p on the deuteron and proton, respectively, from the relation

$$\sigma_n=\frac{\sigma_d-\sigma_p}{1-(\sigma_p/4\pi)\langle 1/r_d^2\rangle},$$

where the mean inverse-square radius of the deuteron, $\langle 1/r_d^2\rangle$, is taken to be $(1/1.7)^2$ f^{-2}. Typically, this correction amounted to 10% of the difference $\sigma_d-\sigma_p$.

The errors quoted in Table I include the statistical errors for the numbers counted and the estimated errors for the corrections (b) and (c) above. Corrections (a) and (d) are assumed to be the best estimates one can apply at present and their uncertainty is unknown. The fluctuation among subgroups of the data was used to estimate the statistical part of the error, and generally gave an answer about 30% higher than that estimated by using the total numbers and assuming random count distributions.

However, apart from the random errors described in the preceding paragraph, a further systematic error

[5] R. J. Glauber, Phys. Rev. **100**, 242 (1955).

of 1 mb must be included. The cross sections deduced from the three counters T_1, T_2, and T_3 systematically disagreed by about this amount, the values decreasing with increasing size of counter. This effect is not completely understood, though part is certainly attributable to the fact that correction (b) for forward scattering, which is proportional to the counter size, is known to have been underestimated. Thus, in determining the shape of the cross-section behavior from the results of Table I, the errors given may be legitimately used, but it should be borne in mind that the absolute normalization of the curve is uncertain by about 2 to 3%.

IV. DISCUSSION

The cross-section results described in the preceding section are plotted in Fig. 5 together with other data at high energies from Cook *et al.*,[1] and at lower energies from bubble chamber measurements.[6]

The new data clearly show a large peak in σ_p, at about 1000 Mev/c, that is approximately ± 100 Mev/c in width. If a smooth curve is interpolated between the regions from 600 to 700 Mev/c and from 1200 to 1300 Mev/c, the peak appears to extend some 15 mb above this "background" value. For convenience, this sharp enhancement at 1000 Mev/c will be loosely referred to below as a resonance.

If one assumes charge independence for the K-nucleon interaction, i.e., that the interaction is completely specified by the two cross sections σ_0 and σ_1 corresponding to the $I=0$ and $I=1$ states, it follows that $\sigma_n=\sigma_1$ and $\sigma_p=\frac{1}{2}(\sigma_0+\sigma_1)$. Thus any structure in the $I=1$ state should be twice as evident in the K^--n as in the K^--p interaction, whereas interactions in the $I=0$ state should reveal themselves only in the K^--p system. Although the data could indicate a broad peaking of σ_n in the neighborhood of 1 Bev/c, it seems very unlikely that there could be a peak some 30 mb above a smooth background, which would be necessary if the resonance in σ_p were wholly in the $I=1$ state. Thus, the data are consistent with the interpretation of the resonance as being largely in the $I=0$ state.

The simplest explanation of the peak is in terms of a resonance in a single state of well-defined angular momentum, parity, and isotopic spin. Examining the maximum effect from different partial waves at 1 Bev/c, one finds that the most a $J=\frac{1}{2}$ state can contribute to σ_0 or σ_1 is 18 mb. If this is confined to just a single isotopic-spin state, then the maximum contribution to σ_p becomes 9 mb. Thus it seems necessary to attribute the resonance to a state of $J\geqslant\frac{3}{2}$. In discussing the possibility of a single-state $I=0$ resonance at 1 Bev/c, it should be kept in mind that this would still describe only part of the interaction at this energy, since there is clearly a large nonresonant background (about 35 mb). Also, only a sudden change in σ_0 is considered here because it is clear from a comparison of σ_p and σ_n that σ_1 and σ_0 vary differently with energy.

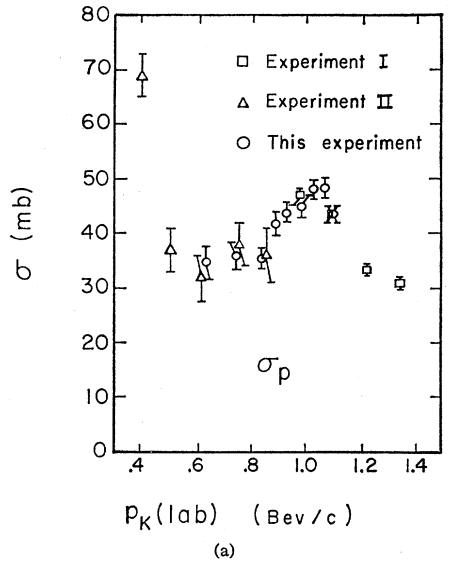

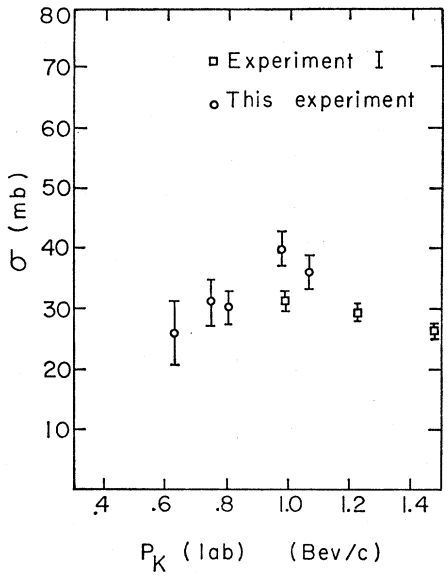

FIG. 5. The total cross sections σ_n and σ_p. Figure 5(a) gives σ_p and 5(b) gives σ_n. Experiment I refers to the experiment of Cook *et al.*[1] and Experiment II refers to the experiment of Bastien *et al.*[6] Points from the present experiment are plotted together with the errors as given in Table I and discussed in the text. In addition, systematic errors of less than 1 mb may be present, which could shift the central values of all points together. (See Sec. III.)

[6] P. Bastien, J. P. Berge, O. Dahl, M. Ferro-Luzzi, W. Humphrey, J. Kirz, D. H. Miller, J. J. Murray, A. H. Rosenfeld, M. Ross, J. A. Schwartz, F. Solmitz, R. Tripp, and M. Watson (unpublished). Preliminary cross-section data from this group have been reported by M. Ferro-Luzzi, Revs. Modern Phys. **33**, 416 (1961).

The difference in the energy dependence of σ_0 and σ_1 at higher energies has been described by Cook *et al.*[1]

Apart from these tentative considerations of the quantum numbers associated with the peak, it is probably more interesting, and heuristically more useful, to discuss the significance of the energy value at which the resonance occurs. There are two reasons, of current interest, for believing that structure in σ_p could occur at about 1000 to 1050 Mev/c:

(a) Global symmetry implies that resonances should exist in the π-Λ and π-Σ systems analogous to those in the π-N system. In particular, the third resonance in the π^--p system in the $I=\frac{1}{2}$ state (total energy in c.m. system equal to 1670 Mev) leads to a prediction of two resonances in the π-hyperon and hence the K^--N system: one with $I=0$ at $p_K=1140$ Mev/c, the other with $I=1$ at $p_K=1310$ Mev/c. The first of these lies at higher energy and should be narrower than the observed resonance,[7] but such discrepancies need not imply disagreement with the idea of global symmetry, in view of the approximate nature of the scheme. However, no evidence for the broader $I=1$ component was found in the work of Cook *et al.*[1]

(b) It may be that the structure in σ_p is associated with the opening of new absorption channels. Several thresholds for new production processes occur in the region of 1040 Mev/c. The reaction $\bar{K}+N \rightarrow K+\Xi$ is known to have a cross section much less than a millibarn at 1.15 Bev/c,[8] and seems very unlikely to have any appreciable effect at 1040 Mev/c. One recently discovered reaction, $\bar{K}+N-\bar{K}^*+N$,[9] has a threshold almost exactly at the resonant energy; the excitation function for this process is not known, but $\bar{K}^*$ production at 1.15 Bev/c amounts to a few millibarns. Other possibly strong reactions at about this energy can be written which involve production of two and three pions, or higher excited-hyperon resonances analogous to the Y^*.[10] Recently Ball and Frazer[11] have shown by a dispersion-theoretic approach how a rapid rise in inelastic absorption in a given state (e.g., close to a threshold) can generate a large and temporary increase in the elastic scattering arising from the same state. From their dispersion relation between the real and imaginary parts of the phase shift in a given state, they show that even for an inelastic cross section of only a few millibarns the elastic cross section in the same state can be induced to rise to the unitarity limit. The peak in the total cross section should occur close to the inelastic threshold, If this is the mechanism involved in the present case it is susceptible to a direct experimental test, because the elastic and inelastic channel could be clearly associated as occurring with the same quantum numbers.

For the specific assumptions of $J=1$ and $I=\frac{1}{2}$ for the $\bar{K}^*$, Ball and Frazer[11] calculate from their model that the peaking in the cross section in the K^--p system should be about five times as great as in the K^--n system. The Fermi momentum of the neutron in the deuteron causes a broadening of the peak; if one assumes projected deuteron momenta of the order of 50 Mev/c, the half-width should be increased by about 20%. The present data on σ_n are not of sufficient statistical accuracy to allow us to decide whether such a reduced and broadened peak exists in σ_n, but they are certainly consistent with the prediction of Ball and Frazer.[11]

ACKNOWLEDGMENTS

We are grateful to Dr. Edward J. Lofgren and the Operations Group of the bevatron, and also to Dr. Carl M. York for help during the course of the experiment. For assistance in setting up and running the experiment, we thank Fred Betz, Helmut Dost, David Linn, Robert Shafer, William Troka, and Shinjiro Yasumi. One of us (A.L.) was partially supported by a National Science Foundation Science Faculty fellowship.

[7] L. T. Kerth and A. Pais, University of California, Lawrence Radiation Laboratory Report UCRL-9706, 1961 (unpublished).
[8] W. B. Fowler, R. W. Birge, P. Eberhard, R. Ely, M. L. Good, W. M. Powell, and H. K. Ticho, Phys. Rev. Letters **6**, 134 (1961).
[9] M. Alston, L. Alvarez, P. Eberhard, M. Good, W. Graziano, H. Ticho, and S. Wojcicki, Phys. Rev. Letters **6**, 300 (1961).
[10] M. Alston, L. Alvarez, P. Eberhard, W. Graziano, M. Good, H. Ticho, and S. Wojcicki, Phys. Rev. Letters **5**, 520 (1960).
[11] J. S. Ball and W. R. Frazer, Phys. Rev. Letters **7**, 204 (1961).